Evaluation of Outcomes After Interventional Procedures

6

Teruomi Miyazawa and Hiroki Nishine

Interventional Procedure

Inoperable central airway stenosis due to a malignant tumor is a relatively common condition and may be life threatening. Because of the poor prognosis, palliative methods are needed to maintain airway patency. In patients with severe malignant airway stenosis, interventional bronchoscopy is considered as a method of maintaining airway patency [1].

Flow limitation during forced expiration is affected by the relationship between transmural pressure (P_{tm}) and the cross-sectional area (A) of the airway. The wave speed is dependent on the stiffness of the airway wall, i.e., dP_{tm}/dA, and on the cross-sectional airway itself [2, 3]. The flow-limiting segment (FLS) occurs originally where the cross-sectional area of the airway is the narrowest. On the basis of wave-speed concepts of maximal expiratory flow limitation, stenting at the FLS improved expiratory flow limitation by increasing the cross-sectional area, supporting the weakened airway wall and relieving dyspnea [4, 5].

Assessment of Flow–Volume Curve

The location of the FLS is assessed using flow–volume curves. Analysis of the flow–volume curve can be used to define the nature of the stenosis and provide reliable information on the efficacy of stenting [5–10]. In patients with tracheal stenosis, the flow–volume curve shows a marked reduction of the expiratory flow (fixed narrowing patterns) with a plateau. In patients with bronchial stenosis, the flow–volume curve shows decreased flow with expiratory choking (initial transient peak flow followed by acute flow deterioration and consecutive low flow and dynamic collapse patterns). In patients with carinal stenosis, the flow–volume curve shows a descending expiratory limb with a plateau and choking (combined fixed and dynamic patterns). In patients with extensive stenosis from the trachea and carina, extending to the bronchi due to tumor and/or mediastinal lymphadenopathy, the flow–volume curve shows severe reduction of the expiratory flow (complex patterns containing elements of all the former).

T. Miyazawa, MD (✉) • H. Nishine, MD
Division of Respiratory and Infectious Disease, Department of Internal Medicine, St Mariana University School of Medicine, Sugao Miyamae-ku, Kawasaki, Kanagawa, Japan
e-mail: t.miyazawa@go5.enjoy.ne.jp

J.P. Díaz-Jimenez, A.N. Rodriguez (eds.), *Interventions in Pulmonary Medicine*,
https://doi.org/10.1007/978-3-319-58036-4_6

Dyspnea

The degree of dyspnea depends on the degree of airway obstruction and becomes severe when well over 70% of the tracheal lumen is obstructed [11]. In cases with 50% *tracheal obstruction*, the highest velocities are in the jet, which is generated by glottic constriction. In cases with over 70% *tracheal obstruction*, peak velocities are generated at the stenosis and exceed velocities in the glottic area. Pressure differences changed dramatically from 70% *tracheal obstruction*.

The relation between the baseline degree of *tracheal obstruction* and the changes in MMRC (ΔMMRC) is shown in Table 6.1. Any patient with an improvement in the MMRC scale of 2 or more was considered to be a clinical responder. The clinical responder rate was 84.6% for obstructions above 80 and 58.8% for obstructions between 50 and 80%. Preoperation measures by the baseline degree of *tracheal obstruction* could be used to predict the postoperation impact on dyspnea [12].

Assessment of Lateral Airway Pressure

Analysis of the flow–volume curve could be used in defining the nature of the stenosis. However, flow–volume curves cannot identify the precise location of the lesion where airway resistance increases, nor can it immediately define the outcome of stenting.

With the use of airway catheters in dogs [13–15] and in human subjects [16–18], the FLS could be located by measuring lateral airway pressure (P_{lat}) during induced flow limitation generated by either an increase in pleural pressure or a decrease in downstream pressure. Healthy subjects have relatively uniform pressure drop down of the bronchial tree during expiration. In patients with airway stenosis, the major pressure drop occurs across the stenosis. By measuring P_{lat} on each side of the stenosis, we could detect the pressure difference between two sites (proximal and distal) of the stenotic segment [12].

After intubation, a double lumen airway catheter was inserted into the trachea during bronchoscopy. P_{lat} was measured simultaneously at two points during spontaneous breathing with light general anesthesia before and after intervention. P_{lat} at the two points was plotted on an oscilloscope (pressure–pressure (P–P) curve). The angle of the P–P curve was defined as the angle between the peak inspiratory and expiratory pressure points and the baseline of the angle. If the cross-sectional area (CSA) was small, then the angle was close to 0°; however, after intervention, the CSA significantly increased and the angle was close to 45°.

In healthy subjects, no pressure difference between the carina and trachea was observed (0.10 ± 0.22 cm H_2O) during tidal breathing (Fig. 6.1a). The P–P curves were linear and the angle of the P–P curve was close to 45° (44.6 ± 0.98) (Fig. 6.1b).

In patients with *tracheal obstruction*, dyspnea scale, pressure difference, and the angle changed significantly beyond 50% obstruction (Fig. 6.2a, b). After stenting, the pressure difference disappeared and the angle was close to 45°. The degree of *tracheal obstruction* was significantly correlated with the pressure difference and the angle ($r = 0.83$, $p < 0.0001$, and $r = -0.84$, $p < 0.0001$, respectively) [12].

Table 6.1 Relation between the baseline degree of *tracheal obstruction* and the change in MMRC after interventional bronchoscopy

Degree of tracheal obstruction (%)	ΔMMRC[a]		Responders[b] (%)
	≦1	≧2	
51–60		2	
61–70	2	2	10/17 (58.8%)
71–80	5	6	
81–90	2	9	11/13 (8406%)
91–100		2	

[a]ΔMMRC = change in MMRC scale
[b]ΔMMRC responder = improvement in MMRC scale of 2 or more

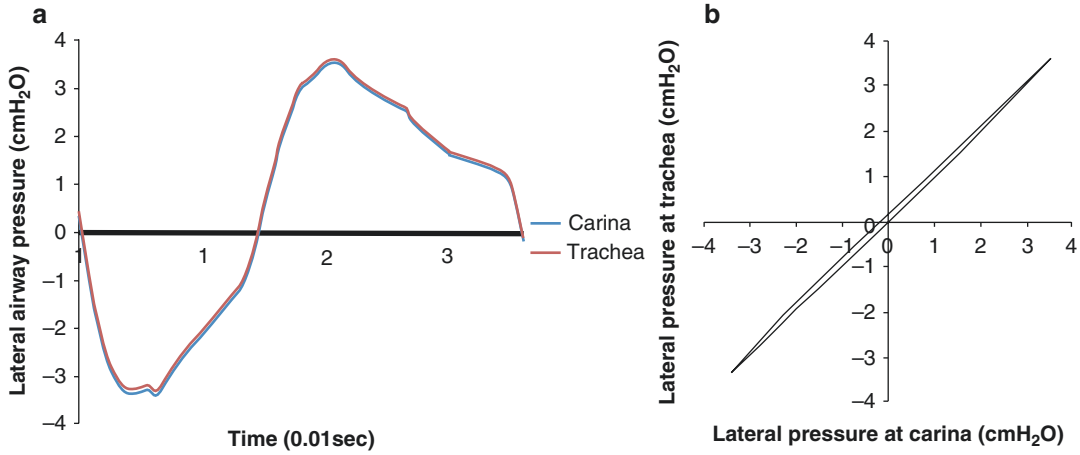

Fig. 6.1 Typical patterns of lateral airway pressure (P_{lat}) measurements during tidal breathing in a *healthy subject*. P_{lat} is measured simultaneously at two points (upper trachea and carina). There are no pressure differences between the carina and upper trachea (**a**). (*Blue*, carina; *red*, upper trachea.) The angle of pressure–pressure (P–P) curve is defined as the angle between peak inspiratory and expiratory pressure points and the baseline of the angle. The P–P curves are linear and the angle of P–P curve is close to 45° (**b**)

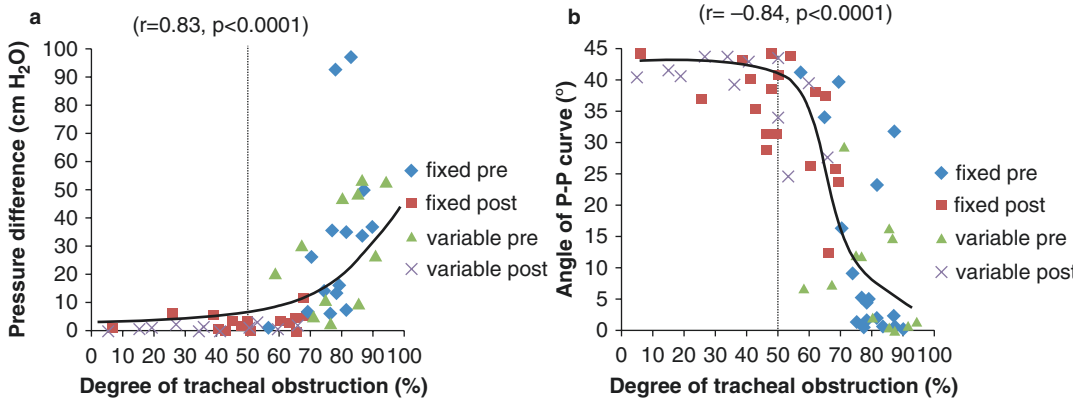

Fig. 6.2 Scatter plot of pressure difference and the angle of the pressure–pressure (P–P) curve versus the degree of *tracheal obstruction*. *Blue diamonds* show before intervention and *red squares* indicate after intervention in cases with *fixed stenosis*. *Green triangles* show before intervention and *purple Xs* indicate after intervention in cases with *variable stenosis*. *Dotted line* shows the threshold for 50% *tracheal obstruction*. The pressure difference (**a**) and the angle of P–P curves (**b**) are significantly correlated with the degree of *tracheal obstruction*. The pressure difference increased significantly above 50% obstruction (**a**). When the cross-sectional area was small, the angle of the P–P curve was close to 0°. After interventional bronchoscopy, the cross-sectional area increased and the angle of the P–P curve was close to 45° (**b**)

This approach identified a need for additional treatment during interventional bronchoscopy. In a patient with *fixed intrathoracic stenosis* due to tracheal tuberculosis, CT showed a tracheal stenosis at the middle trachea (Fig 6.3a). Before treatment, a considerable pressure difference between the upper trachea and carina was noted (Fig. 6.3d), and the angle of the P–P curve was 0.3° (Fig. 6.3i). The flow–volume curve shows marked reduction of the expiratory and inspiratory

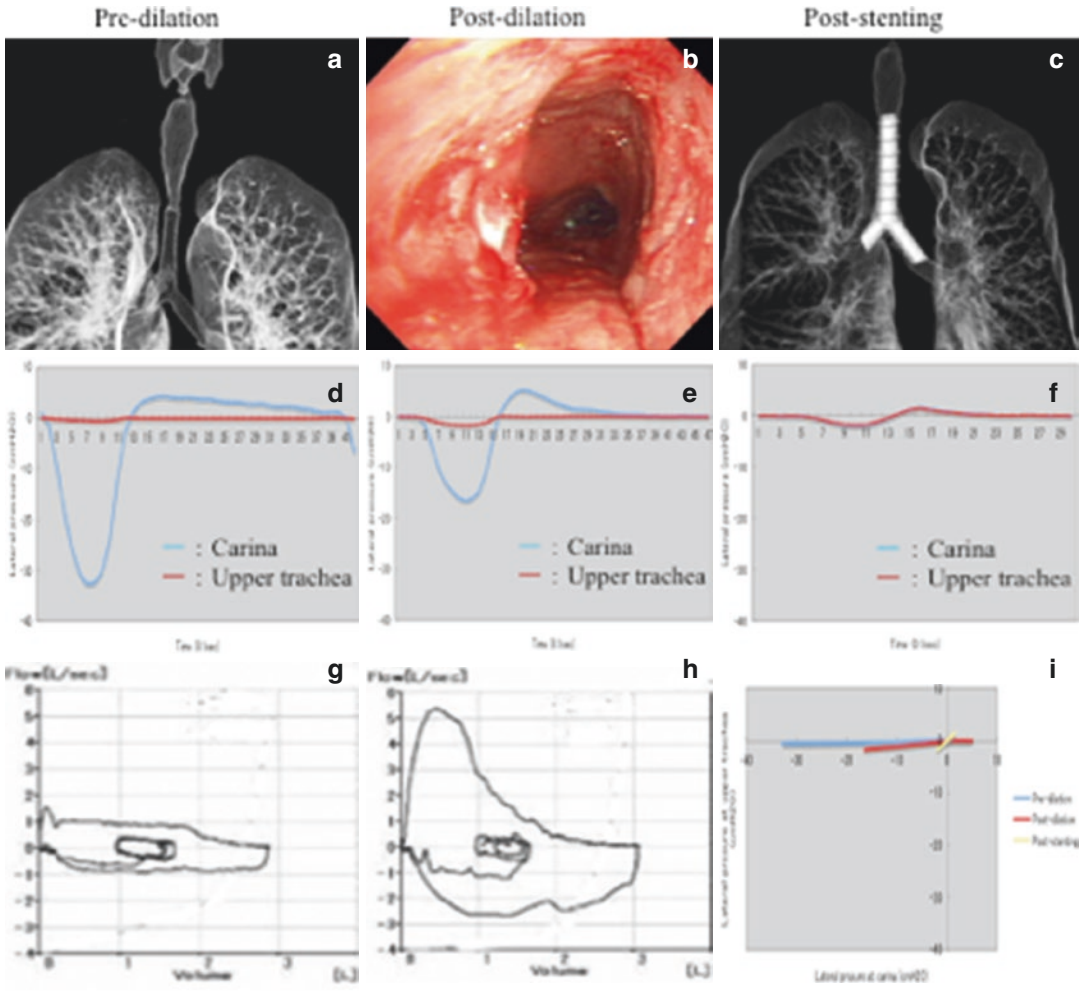

Fig. 6.3 Lateral airway pressure (P_{lat}) measurements during interventional bronchoscopy with balloon dilation and silicone Y stent implantation in *fixed intrathoracic stenosis* due to tracheal tuberculosis (before treatment, *panels* (**a**, **d**, and **g**); after balloon dilation, *panels* (**b** and **e**); after stenting, *panels* (**c**, **f,** and **h**)). P_{lat} was measured simultaneously at two points (the upper trachea and carina). *Blue line* shows P_{lat} at carina and the *red line* indicates P_{lat} at upper trachea (**d–f**). After each treatment, the angle of P–P curve showed a stepwise improvement over the interventional procedures (**i**). See text for further explanation

flow (Fig. 6.3g). After balloon dilation, bronchoscopic imaging revealed greater patency for the trachea (Fig. 6.3b). However, the pressure difference only decreased from 36.6 to 20.1 cmH_2O (Fig. 6.3e), and the angle of the P–P curve only increased from 0.3° to 5.0° (Fig. 6.3i). Subsequently, a silicone Y stent was implanted from the upper trachea to the both main stem bronchi. After stenting (Fig. 6.3c), pressure differences disappeared (Fig. 6.3f), and the angle of the P–P curve increased from 5.0° to 35.8° (Fig. 6.3i). The MMRC scale decreased from 2 to 0 and flow–volume curve returned to a near-normal pattern (Fig. 6.3h). Measuring P_{lat} could estimate the need for additional procedures better than bronchoscopy alone. The direct measurement of the pressure difference and the angle of pressure–pressure curve is a new assessment modality for the success of interventional bronchoscopy.

Analysis of Pressure–Pressure Curve

Central airway stenosis can be divided into four major types: *fixed*, *variable*, *extrathoracic*, and *intrathoracic stenosis*. In *fixed stenosis*, the CSA at the site of the lesion does not change during the respiratory cycle, and the P–P curve was linear. In *variable stenosis*, the configuration of the stenotic lesion changes between phases of respiration. Airway narrowing occurs during expiration in *intrathoracic stenosis*, whereas airway narrowing occurs during inspiration in *extrathoracic stenosis*. In *variable extrathoracic stenosis*, the angle of the P–P curve during inspiration is smaller than during expiration, and in *variable intrathoracic stenosis*, the angle of the P–P curve during expiration is smaller than during inspiration.

Conclusions

Placement of the stent at the flow-limiting segment (FLS) provided the greatest functional benefit to patients with central airway stenosis [4, 5]. Although bronchoscopic imaging showed that tracheal patency was restored after procedures, the angle of P–P curve did not always improve. It is difficult to estimate the outcome of interventional procedures by bronchoscopy alone. When the location of the FLS is assessed using flow–volume curves, the pressure difference and the angle of pressure–pressure curve are able to immediately estimate the outcomes of interventional bronchoscopy in real time.

References

1. Seijo LM, Sterman DH. Interventional pulmonology. N Engl J Med. 2001;344:740–9.
2. Dawson SV, Elliott EA. Wave-speed limitation on expiratory flow a unifying concept. J Appl Physiol. 1977;43:498–515.
3. Mead J. Expiratory flow limitation: a physiologist's point of view. Fed Proc. 1980;39:2771–5.
4. Miyazawa T, Yamakido M, Ikeda S, Furukawa K, Takiguchi Y, Tada H, Shirakusa T. Implantation of Ultraflex nitinol stents in malignant tracheobronchial stenoses. Chest. 2000;118:959–65.
5. Miyazawa T, Miyazu Y, Iwamoto Y, Ishida A, Kanoh K, Sumiyoshi H, Doi M, Kurimoto N. Stenting at the flow–limiting segment in tracheobronchial stenosis due to lung cancer. Am J Respir Crit Care Med. 2004;169:1096–102.
6. OF P, Ingram RH Jr. Configuration of maximum expiratory flow-volume curve: model experiments with physiological implications. J Appl Physiol. 1985;58:1305–13.
7. Ohya N, Huang J, Fukunaga T, Toga H. Airway pressure-volume curve estimated by flow interruption during forced expiration. J Appl Physiol. 1989;67:2631–8.
8. OF P. The Peak Flow Working Group: physiological determinants of peak expiratory flow. Eur Respir J. 1997;10:11–6.
9. Aljuri N, Freitag L, Vegegas JG. Modeling expiratory flow from excised tracheal tube law. J Appl Physiol. 1999;87:1973–80.
10. Miller RD, Hyatt RE. Evaluation of obstructing lesions of the trachea and larynx by flow-volume loops. Am Rev Respir Dis. 1973;108:475–81.
11. Brouns M, Jayaraju ST, Lacor C, Mey JD, Noppen M, Vincken W, Verbanck S. Tracheal stenosis: a flow dynamics study. J Appl Physiol. 2007;102:1178–84.
12. Nishine H, Hiramoto T, Kida H, Matsuoka S, Mineshita M, Kurimoto N, Miyazawa T. Assessing the site of maximum obstruction in the trachea using lateral pressure measurement during bronchoscopy. Am J Respir Crit Care Med. 2011;185:24–33.
13. Mink S, Ziesmann M, Wood JDH. Mechanisms of increased maximum expiratory flow during HeO_2 breathing in dogs. J Appl Physiol. 1979;47:490–502.
14. Smaldone GC, Itoh H, Swift DL, Wagner HN. Effect of flow-limiting segments and cough on particle deposition and mucociliary clearance in the lung. Am Rev Respir Dis. 1979;120:747–58.
15. OF P, Thiessen B, Lyager S. Airway compliance and flow limitation during forced expiration in dogs. J Appl Physiol. 1982;52:357–69.
16. Macklem PT, Fraser RG, Bates DV. Bronchial pressures and dimensions in health and obstructive airway disease. J Appl Physiol. 1963;18:699–706.
17. Smaldone GC, Smith PL. Location of flow-limiting segments via airway catheters near residual volume in humans. J Appl Physiol. 1985;59:502–8.
18. OF P, Brackel HJ, Bogaard JM, Kerrebijn KF. Wave-speed-determined flow limitation at peak flow in normal and asthmatic subjects. J Appl Physiol. 1997;83:1721–32.